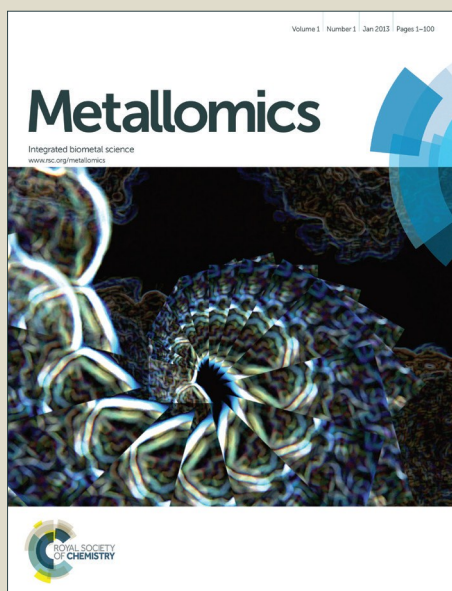# Metallomics

Accepted Manuscript

This is an *Accepted Manuscript*, which has been through the Royal Society of Chemistry peer review process and has been accepted for publication.

Accepted Manuscripts are published online shortly after acceptance, before technical editing, formatting and proof reading. Using this free service, authors can make their results available to the community, in citable form, before we publish the edited article. We will replace this *Accepted Manuscript* with the edited and formatted *Advance Article* as soon as it is available.

You can find more information about *Accepted Manuscripts* in the Information for Authors.

ROYAL SOCIETY OF CHEMISTRY

www.rsc.org/metallomics

Metallomics

ARTICLE

On-line coupling of continuous-flow gel electrophoresis with inductively coupled plasma-mass spectrometry to quantitatively evaluate intracellular metal binding properties of metallochaperones *Hp*HypA and *Hp*HspA in *E. coli* cells

Yuchuan Wang, Ligang Hu, Xinming Yang, Yuen-Yan Chang, Xuqiao Hu, Hongyan Li and Hongzhe Sun*[a]

On-line coupling of gel electrophoresis with inductively coupled plasma-mass spectrometry (GE-ICP-MS) offers a strategy to monitor intracellular metals and their associated proteins simultaneously. Herein, we examine the feasibility of the GE-ICP-MS system in quantitative analysis of intracellular metal binding properties using two *Helicobacter pylori* metallochaperones HypA and HspA overexpressed in *E. coli* cells as a showcase. We show that parallel detection of metal and sulfur signals allows accurate quantification of intracellular metal-protein stoichiometries, even for metalloproteins that bind metal ions with micromolar affinities. Using this approach, we demonstrate that only trace amounts of Ni^{2+} associated with *Hp*HypA in cells, distinct from *in vitro* observation of stoichiometric binding, while *Hp*HypA exhibits a high fidelity towards its structural metal Zn^{2+} with stoichiometric Zn^{2+} binding. In contrast, *Hp*HspA associates with Zn^{2+}, Ni^{2+}, Cu^{2+} and Co^{2+} from an essential metal pool with *ca.* 0.5 molar equivalents of total metals bound per *Hp*HspA monomer. The metal binding properties of both *Hp*HypA and *Hp*HspA were altered by Bi^{3+}. Bindings of both Zn^{2+} and Ni^{2+} to *Hp*HypA were suppressed under the stress of Bi^{3+} in cells, different from *in vitro* studies that Bi^{3+} only interfered with Zn^{2+} but not Ni^{2+} binding. This study provides an analytical approach to investigate intracellular metal selectivity of overexpressed metalloproteins.

Introduction

Quantification of metal-protein binding in cells will help to quickly identify the metals that bind to metalloproteins under physiologically relevant conditions, providing invaluable information to comparatively assess metalloproteome dynamics upon external stimuli.[1, 2] However, there appear very limited approaches to allow quantification of metals bound to metalloproteins in cells due to the complexity of the cellular environment, and the non-covalent metal-protein binding makes it even more challenging. We have previously developed a robust and convenient method to match metals to their bound proteins in cells by integration of column-type gel electrophoresis (GE) with inductively coupled plasma-mass spectrometry (ICP-MS).[3] Such a strategy (GE-ICP-MS) offers simultaneous identification of all relevant metals associated with the protein of interest at a metallome-wide scale, with sensitivity at the femtomole level.

Metallochaperones play essential roles in cellular metal homeostasis by assisting metal trafficking *via* specific protein-protein interactions, and ultimately facilitate maturation of metalloenzymes.[4-6] Increasing evidences suggest that proteins involved in metal homeostasis might be attractive drug targets, as some metallodrugs have been demonstrated to bind directly to metallochaperones,[7-10] thus inhibiting their metal chaperone activities and disrupting functions of key enzymes. Ni^{2+} chaperone HypA from *Helicobacter pylori* plays crucial roles in the maturation of two enzymes i.e. [Ni, Fe]-hydrogenase and urease. Proper functions of these enzymes are critical for the pathogenesis of the stomach bacterium.[11] *Hp*HypA contains a high affinity Zn^{2+} site playing a structural role, and a low affinity Ni^{2+} site communicating with potential Ni^{2+} delivery proteins such as HypB or UreE in cells.[12-15] Metallochaperone HspA is an indispensable chaperonin in *H. pylori* with a unique histidine- and cysteine-rich C-terminus involved in Ni^{2+} sequestration,[16, 17] and was identified as a potential bismuth-based drug target in the

pathogen.[18] The protein might associate with multiple transition metals and participate in metal homeostasis other than Ni^{2+} in *H. pylori*, resembling *H. pylori* and *E. coli* SlyD that binds various metal ions *via* similar metal binding domains.[19, 20]

In this work, we first validated GE-ICP-MS in quantitative analysis of metal binding properties of proteins in cells. We then applied this strategy to examine the intracellular metal selectivity of *H. pylori* metallochaperones HypA and HspA overexpressed in *E. coli* cells, which was compared with those observed *in vitro*. The effects of bismuth on metal binding properties of the two metallochaperones were also investigated in cells and *in vitro*. This study demonstrates the feasibility of GE-ICP-MS in examination of metal-protein interactions in cells.

Materials and methods

Bacterial strains and molecular cloning

Helicobacter pylori 26695 was obtained from American type culture collection (ATCC 700392). The *hypA* and *hspA* genes were cloned and amplified from the genomic DNA of *H. pylori* 26695. All plasmids used were maintained in *E. coli* XL-1 Blue cells (Stratagene), and *E. coli* BL21 (DE3) cells (Stratagene) were used for protein overexpression. The details on DNA manipulation were reported previously.[12, 16] After DNA purification (GE), the PCR products were ligated into a pET32a vector with T4 DNA ligase (New England Biolabs). All the DNA constructs were transformed into XL-1 Blue *E. coli* cells and verified by DNA sequencing (Invitrogen).

Preparation of purified Zn, Ni-*Hp*HypA and Zn-RING

The *Hp*HypA and XIAP-RING were expressed and purified similarly as previously described.[12, 21] Protein concentrations were determined using the Bradford protein assay (Bio-rad) with BSA as a standard. To obtain Zn^{2+} and Ni^{2+} fully loaded *Hp*HypA (Zn, Ni-*Hp*HypA) and Zn^{2+} fully loaded RING (Zn-RING), freshly prepared *Hp*HypA or RING was incubated with 10-fold molar excesses of Zn^{2+} and Ni^{2+} for *Hp*HypA or Ni^{2+} only for RING overnight at 4°C. The unbound metal ions were removed by ultrafiltration using size exclusive membranes (Amicon Ultra, 3 kDa cut-off, Millipore) and buffer exchanged five times (concentrated 10-fold each time) into Tris buffer (20 mM Tris, 100 mM NaCl, 1 mM TCEP, pH 7.4).

Determination of whole-cell metal accumulation and preparation of cytosolic proteins

E. coli BL21 (DE3) cells harboring the expression plasmid pET32a-*hypA* or pET32a-*hspA* were cultured in M9 minimal medium with the supplementation of respective metal mixtures (10 μM of each metal was supplemented unless otherwise specified). The metal salts including $MnCl_2 \cdot 4H_2O$, $FeCl_3$, $CoCl_2 \cdot 6H_2O$, $NiSO_4 \cdot 6H_2O$, $CuCl_2 \cdot 2H_2O$, $ZnSO_4 \cdot 7H_2O$ and $Na_2MoO_4 \cdot 2H_2O$ were used as the essential metal sources and colloidal bismuth subcitrate (CBS, Livzon Pharmaceutical Group) or Bi-NTA as the Bi^{3+} sources. Protein overexpression was induced by simultaneous addition of 0.2 mM IPTG and metals of interest, followed by further incubation for 12 h at 25°C. Cell densities (OD_{600}) were recorded prior to harvesting. Cells were washed by chilled Tris buffer containing 1 mM EDTA for three times and then three times with the same Tris buffer without EDTA. Half of the bacterial pellets were desiccated at 60°C for 48 h and the dry cells were weighted, the pellets were

then digested in 70% HNO_3 and diluted to a final concentration of 5% HNO_3 for ICP-MS analysis.

For cytosolic proteins, the remaining pellets were lysed by sonication at 4°C in Tris buffer containing 5 mM TCEP and ultracentrifuged (15,000 g, 30 min at 4°C) to remove cell debris. The supernatants containing bacterial cytosolic and periplasmic proteins were separated by native-PAGE (Fig. S1-S2) to verify the successful overexpression of the proteins.

GE-ICP-MS measurement

GE-ICP-MS system was used to monitor the metals associated with overexpressed proteins in cells. The experimental details were the same as described previously.[3] Briefly, a modified column gel electrophoresis separation system (Bio-rad) was coupled with an ICP-MS spectrometer (Agilent 7500a, Agilent Technologies, CA, USA) for specific metal analysis. A 3.0 cm long native gel was casted to the gel column (8% and 15% gel was used for the separation of *Hp*HspA and *Hp*HypA protein lysates respectively), with a 0.5 cm long 4% native gel stacking on top. Tris-glycine running buffer (25 mM Tris, 192 mM glycine, pH 8.3) was applied to the gel electrophoresis system as recommended, with 50 mM ammonium nitrate buffer transferring the eluted protein solution to ICP-MS. Operating parameters of the ICP-MS spectrometer are summarized in Table S1. Elements of interest are ^{34}S, ^{55}Mn, ^{57}Fe, ^{59}Co, ^{60}Ni, ^{63}Cu, ^{66}Zn, ^{95}Mo and ^{209}Bi (Fig. S5). For protein identification, a T-connection tubing was employed to split the solution after electrophoresis separation, transferring half of the solution to a collection tube. Gel electrophoresis was performed using a consecutive three-step voltage program (10 min at 100 V, 90 min at 200 V and 500 V till the end), where the metal-binding proteins were eluted at the last step.

Peptide mass fingerprint

Protein fractions corresponding to the major metal peaks during GE-ICP-MS analysis were collected and identified through peptide mass fingerprinting. The collected fractions were concentrated *via* ultrafiltration (Amicon Ultra, 3 kDa cut-off, Millipore) and separated by Native-PAGE (Fig. S6). Protein spots of interest were excised from the silver-stained gels. After gel destaining and washing, samples were digested overnight with trypsin at 37°C. The digested peptides were desalted by Ziptip and dissolved in 0.1% formic acid, 50% acetonitrile solution. The molecular masses were determined by MALDI-TOF/TOF-MS analysis. The data were searched against NCBInr protein database using MASCOT searching engine.

Results

Quantification of metalloproteins by GE-ICP-MS

Maintaining the integrity of metal-protein complex is a prerequisite for accurate metal quantification in GE-separation-based metalloprotein analysis.[22] We first evaluated the feasibility of using GE-ICP-MS to quantify metalloproteins in cells. All gel electrophoresis (GE) separations in this work were carried out under non-denaturing conditions and HypA from *H. pylori* was chosen as a showcase study as it binds Zn^{2+} and Ni^{2+} at specific sites.[12] *Hp*HypA was overexpressed and purified as described previously,[12] and was loaded with one molar equivalents of Zn^{2+} and Ni^{2+} (Table 1). The same amounts of Zn, Ni-*Hp*HypA were in parallel subjected to GE-ICP-MS and ICP-MS analyses, and monitored in time-resolved analysis (TRA) mode to compare the

Table 1 Analysis of recombinant Zn, Ni-HpHypA by GE-ICP-MS and direct ICP-MS.

M^{2+}-HypA	Metal stoichiometry [a]	Metal content $_{inject}$ (nmol) [b]	Metal content $_{GE}$ (nmol) [b]	Metal recovery (%)	Ratio (M^{2+}/S)$_{inject}$ [c]	Ratio (M^{2+}/S)$_{GE}$ [c]
Zn-HypA	1.12 ± 0.07	1.07 ± 0.09	0.62 ± 0.12	58 ± 4	11.39 ± 0.17	11.33 ± 0.83
Ni-HypA	0.90 ± 0.04	0.86 ± 0.06	0.56 ± 0.15	65 ± 7	13.41 ± 0.05	13.03 ± 1.02

[a] Average metal contents in pure proteins determined by ICP-MS. Protein concentrations were determined by Bradford protein assay. [b] Average metal contents *via* external calibration using ^{66}Zn and ^{60}Ni standard solutions. [c] The ratio was determined from the integrated signal areas of ^{66}Zn or ^{60}Ni versus ^{34}S.

contents of Zn^{2+} and Ni^{2+} detected by both methods. The amounts of bound metals in HpHypA were quantified by an external calibration using a series of diluted ICP standard solutions. About 0.62 ± 0.12 and 0.56 ± 0.15 nmol of Zn^{2+} and Ni^{2+} were detected to bind HpHypA respectively from GE-ICP-MS analysis, but 1.07 ± 0.09 and 0.86 ± 0.06 nmol from ICP-MS analysis. Assuming the amounts of the protein remained unchanged during GE-ICP-MS, the metal recovery percentages for Zn^{2+} and Ni^{2+} were calculated to be (58 ± 4)% and (65 ± 7)% respectively after GE separation (Table 1). This could be either due to dissociation of the metals from the protein or losses of the protein during separation,[23] which was further investigated by monitoring ^{34}S to quantify the protein amounts. The ratios of integrated signal areas of ^{66}Zn to ^{34}S and ^{60}Ni to ^{34}S in both methods were compared, with ^{66}Zn/^{34}S from GE-ICP-MS being 11.33 ± 0.83, comparable to that from ICP-MS (11.39 ± 0.17). Similarly, the ratios of ^{60}Ni/^{34}S are 13.03 ± 1.02 and 13.41 ± 0.05 from GE-ICP-MS and ICP-MS analyses respectively (Table 1), indicating that both Zn^{2+} and Ni^{2+} are well preserved on the protein. However, the losses of the protein for *ca.* 40% were observed during GE separation. A series of Zn, Ni-HpHypA samples at concentrations ranging from 15 to 90 μM were subjected to GE-ICP-MS analysis for further validation (Fig. S3). The levels of ^{66}Zn or ^{60}Ni detected against the amounts loaded gave rise to calibration curves with good linearities (> 0.99) for both metals, further corroborating the well-preserved integrity of metal-protein complexes in GE-ICP-MS analysis (Fig. 1). These results suggest that GE-ICP-MS is applicable for determination of metal-protein stoichiometries providing that the metal and ^{34}S signals are detected simultaneously with the latter being used for protein quantification.

To accurately quantify the amount of HpHypA, a good internal standard, i.e. a protein with a similar structure and metal binding property is desirable.[24] Here, a zinc-saturated XIAP-RING domain protein[25] was employed as an internal standard to quantify intracellular HpHypA amount. Given that the metal-protein stoichiometry remains unchanged during GE-ICP-MS, by determination of metal contents of the analyte and standard proteins, the amounts of both proteins can be deduced. Intact HpHypA and RING exist as a monomer and a dimer with molecular weights of 13.6 and 16.8 kDa respectively. To determine intracellular Zn-HpHypA stoichiometry (as shown in Table 2), HpHypA-overexpressed *E. coli* cell lysates were mixed with purified Zn-RING, and then subjected to GE-ICP-MS analysis using 15% polyacrylamide gel. The amounts of Zn^{2+} bound to HpHypA and RING dimer were first determined by external calibration to be 0.75 nmol and 1.72 nmol respectively. Considering that each RING monomer binds two Zn^{2+} ions and contains 7 Cys and 3 Met residues, the amounts of sulfur in RING dimer were then calculated from the amounts of Zn^{2+} to be 8.62 nmol. Subsequently, the sulfur contents of HpHypA were deduced from the ratio of the integrated signal areas

^{34}S$_{HpHypA}$/^{34}S$_{RING}$ (Fig. S4A) to be 7.68 nmol. Considering that HpHypA contains 6 Cys and 4 Met residues, cellular HpHypA amount was calculated to be 0.77 nmol and the cellular Zn-HpHypA stoichiometry was determined accordingly to be 0.98. All the intracellular metal-HpHypA binding stoichiometries summarized in Table 2 were determined similarly.

As no proper internal protein standards were found for HpHspA, the protein concentration upon GE-ICP-MS analysis was quantified by external ^{34}S calibration using a serial dilution of BSA standard from the commercially available BCA kit (Fig. S4B and Fig. S5). The protein concentrations were then converted by ^{34}S amounts accordingly.
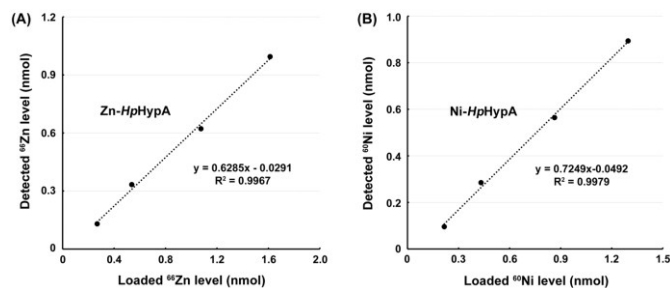

Fig. 1 Calibration curves of ^{66}Zn and ^{60}Ni bound to HpHypA in GE-ICP-MS system. The metal contents detected by GE-ICP-MS are plotted against those loaded. Both curves give rise to good linearities (R^2 > 0.99), indicative of well-preserved integrity of the metal-protein complexation during native GE-ICP-MS analysis.

Intracellular metal selectivity of HpHypA

E. coli cells overexpressing HpHypA were cultured in metal-free M9 medium with the supplementation of metal sources specifically. HpHypA was not successfully overexpressed in the culture medium in the absence of Zn^{2+} (Fig. S1). Upon supplementation of either Zn^{2+} alone or with other essential metals together such as Ni^{2+} or Cu^{2+} in a 1:1 molar ratio (i.e. 10 μM each) to the culture medium, HpHypA was expressed at almost the same levels and showed a high fidelity towards its structural metal by binding with stoichiometric amounts of Zn^{2+} (Table 2). To our surprise, negligible amounts of Ni^{2+} (2% - 3% of the amounts of Zn^{2+}) were detected associating with HpHypA even in the presence of 10-fold molar excess of Ni^{2+} relative to Zn^{2+} (Table 2, Fig. 2B), suggesting that the nickel site of HpHypA is not fully occupied by Ni^{2+} in cells considering that the integrity of Ni-HpHypA remains undisturbed during GE-ICP-MS analysis. Despite that the current study is not carried out in *H. pylori*, given the highly conserved metal binding site of the protein in both microbes, it is reasonable to assume that binding of Ni^{2+} to the protein in *H. pylori* cells is also transient as

Table 2 Metal contents of _Hp_HypA overexpressed in _E. coli_. The data show as an average value with standard deviations derived from triplicate measurements.

Sample	Molar equivalents of metal / HypA			
	Zn^{2+}	Ni^{2+}	Cu^{2+}	Bi^{3+}
HypA-Zn^{2+} (10)	0.98 ± 0.01	ND [a]	ND	ND
HypA-Zn^{2+}, Ni^{2+} (10:10)	1.03 ± 0.06	0.02 ± 0.001	ND	ND
HypA-Zn^{2+}, Ni^{2+} (1:10)	1.03 ± 0.06	0.03 ± 0.01	ND	ND
HypA-Zn^{2+}, Cu^{2+} (10:10)	1.02 ± 0.04	ND	0.04 ± 0.02	ND
HypA-Zn^{2+}, Ni^{2+}, Bi^{3+} (10:10:10)	1.00 ± 0.03	ND	ND	0.17 ± 0.01

[a] ND, non-detectable

intracellular metal selectivity of a metalloprotein may largely depend on the inherent properties of its metal binding sites.[26]
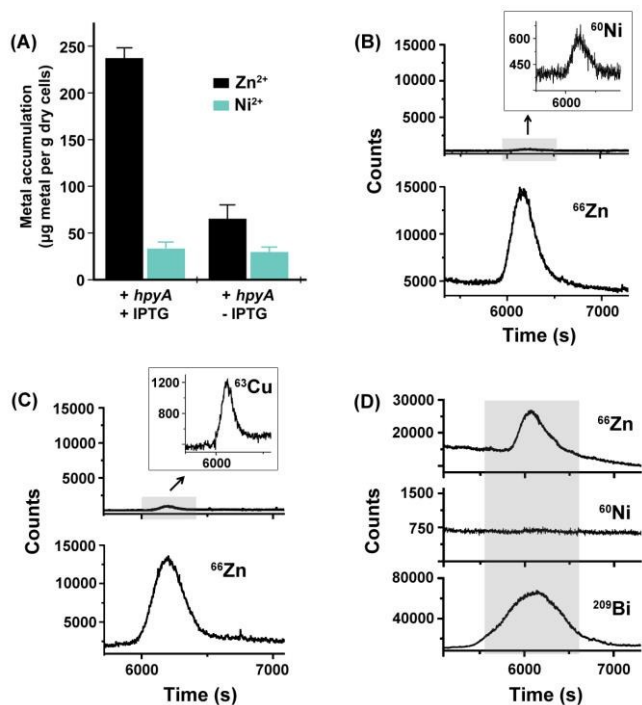

Fig. 2 _Hp_HypA shows a high fidelity towards Zn^{2+} in cells. (A) Metal accumulation in _E. coli_ cells harboring _hypA_ gene. Cells were cultured in M9 medium supplemented with Zn^{2+} and Ni^{2+} (10 μM each), with or without the induction of protein expression. Each column represents the mean ± S.D. from duplicate measurements of at least three independent experiments. (B)-(D) GE-ICP-MS analysis of the _Hp_HypA overexpressed _E. coli_ cell lysates supplied with Zn^{2+}, Ni^{2+} (B) or Zn^{2+}, Cu^{2+} (C) or Zn^{2+}, Ni^{2+}, Bi^{3+} (D). _Insets_ of (B) and (C): Expansions of ICP-MS spectra of ^{60}Ni and ^{63}Cu eluted with the major ^{66}Zn peaks.

To further validate this hypothesis, we determined Zn^{2+} and Ni^{2+} contents accumulated in _E. coli_ cells harboring _hypA_ gene by ICP-MS. As shown in Fig. 2A, an evident increase (_ca_. 2.7 folds) in the amounts of Zn^{2+} was accumulated in the cells overexpressing _Hp_HypA. In contrast, only a slight increase (_ca_. 0.2-fold) in the amounts of Ni^{2+} was noted under the same conditions, indicating that _Hp_HypA was not fully loaded with

Ni^{2+} in cells. These data again suggest a transient metal-protein interaction, which often occurs when the protein plays a role on regulation of metal metabolism.[1] According to Irving-Williams series, copper and zinc are the most competitive among the first row transition metal ions in terms of formation of stable complexes with proteins.[27] Upon supplementation of equimolar amounts of Zn^{2+} and Cu^{2+} to _Hp_HypA overexpressed cells, only 0.04 molar equivalents of Cu^{2+} were detected binding to _Hp_HypA (Table 2, Fig. 2C), in consistent with our observation of high specificity of _Hp_HypA towards its structural metal Zn^{2+} inside cells. Further _in vitro_ examination of Cu-_Hp_HypA interaction indicated that Cu^{2+} binds to the protein _via_ coordinating to histidines (Fig. S7).

To examine the effect of a metallo-agent on the intracellular metal selectivity of _Hp_HypA, gradient concentrations of colloidal bismuth subcitrate (CBS) together with the essential metals (Ni^{2+} and Zn^{2+}, 10 μM each) were supplemented to the culture medium. Upon supplementation of the same amounts of CBS as those essential metal ions to the cells, we observed a broad ^{209}Bi peak with only 0.17 equivalents of Bi^{3+} bound to _Hp_HypA, whereas Ni^{2+} binding to the protein was abolished. In contrast, stoichiometric binding of Zn^{2+} to _Hp_HypA retained (Table 2, Fig. 2D). With Bi^{3+} concentrations increased from 20 to 100 μM, where _Hp_HypA exists as a dimer in the cell lysate (Fig. S8), the majority of Bi^{3+} was detected at the elution time points corresponding to the dimer of _Hp_HypA. Binding of both Ni^{2+} and Zn^{2+} to the protein was completely abolished in the presence of 40 μM Bi^{3+} (Fig. 3B), indicating that Bi^{3+} interferes with binding of both essential metals to the protein in cells and such binding also alters protein quaternary structure.
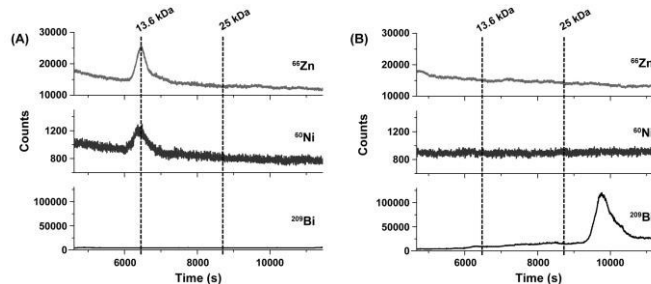

Fig. 3 GE-ICP-MS analysis of the cell lysates supplemented without Bi^{3+} (A) or with 40 μM Bi^{3+} (B) under the conditions similar to the essential metals. The indicated molecular weights were estimated from the elution times of metal-associated _Hp_HypA monomer (13.6 kDa) and _Hp_SlyD monomer (25 kDa) analyzed by GE-ICP-MS under the same gel conditions.

Interaction of recombinant *Hp*HypA with Bi³⁺

To investigate whether bismuth binds to *Hp*HypA at its Zn^{2+} site *in vitro*, Bi-NTA was titrated in a step of 0.2 molar equivalents into 20 μM Zn^{2+} bound *Hp*HypA (Zn-*Hp*HypA) in Hepes buffer containing 1 mM TCEP, pH 7.4, and monitored by UV-vis spectroscopy. As shown in Fig. 4A, a broad absorption band at 360 nm appeared in the UV-vis difference spectra, which is characteristic for bismuth binding to cysteines.[8, 10, 28, 29] The intensity of this band increased with the stepwise addition of Bi-NTA, and leveled off at a molar ratio of [Bi-NTA]/[Zn-*Hp*HypA] of 1.5:1, indicative of binding of 1.5 Bi³⁺ per *Hp*HypA monomer, and possible displacement of Zn^{2+} from the protein by Bi³⁺. The dissociation constant (K_{d1}') of Bi³⁺-*Hp*HypA was calculated to be $6.85(\pm1.49)\times10^{-18}$ μM based on the UV data and known Bi-NTA binding constant ($\log K_a= 17.55$). Apart from four cysteines in the Zn-binding site, *Hp*HypA possesses two additional cysteines (Cys14 and Cys58) within a distance to form a disulfide bond. To investigate if these two cysteines are involved in Bi³⁺ binding, we carried out a similar UV titration experiment except that *Hp*HypA was pretreated with 50-fold hydrogen peroxide (H_2O_2) to oxidize the two cysteines. Despite that the absorption band at 360 nm could still be observed, it leveled off at a molar ratio of [Bi-NTA]/[H_2O_2-treated Zn-HypA] of 1:1 (Fig. 4B), indicating that bismuth still binds the oxidized *Hp*HypA with a slightly lower dissociation constant ($K_{d2}'= 2.96(\pm0.79)\times10^{-18}$ μM). The lower stoichiometry (1:1) of Bi³⁺ binding to H_2O_2 treated Zn-*Hp*HypA suggests that Cys14 and Cys58 also participate in Bi³⁺ binding.

To further examine the effect of Bi³⁺ on Zn^{2+} and Ni^{2+} binding to *Hp*HypA *in vitro*, Zn,Ni-*Hp*HypA was incubated with different molar equivalents of Bi-NTA in the same buffer containing 1 mM TCEP, and then subjected to desalting treatment to remove unbound metal ions, and the bound metals were subsequently quantified by ICP-MS. As shown in Fig. 4C, a gradual increase in amounts of Bi³⁺ binding to *Hp*HypA was accompanied by a decrease in Zn^{2+} binding to the protein and reached a plateau at *ca.* 1.2 Bi³⁺ per monomer of HypA. By contrast, Ni^{2+} binding to the protein was almost undisrupted by Bi³⁺ under identical conditions.

The effect of Bi³⁺ on *Hp*HypA quaternary structure was also investigated by gel filtration chromatography and native gel electrophoresis. As shown in Fig. 4D, upon supplementation of 0, 0.5, 1.0 and 2.0 molar equivalents of Bi³⁺ to Ni, Zn-HypA, a gradual shift of *Hp*HypA elution volumes from 12.1 to 11.8 mL (accompanied by an increase of UV absorbance at 280 nm) was observed, corresponding to monomer and dimer respectively, which was further supported by native gel electrophoresis analysis of Bi³⁺-treated *Hp*HypA (Fig. S9). Binding of Bi³⁺ alters HypA quaternary structure from a native form i.e. monomer[13] to a dimer, which also corroborated our observation on the non-integral binding property. It is likely that Bi³⁺ binds at the Zn^{2+} site and also coordinates to two pairs of Cys14 and Cys58 donated from each monomer, leading to a stoichiometry of [Bi³⁺]/[HypA] of 1.5:1.

The purified Ni, Zn-*Hp*HypA samples incubated with 0, 0.5, 1.0 and 2.0 molar equivalents of Bi-NTA were further subjected to GE-ICP-MS analysis. It is noted that in the absence of Bi³⁺, both Zn^{2+} and Ni^{2+} peaks appeared at elution times corresponding to *Hp*HypA monomers (Fig. S11), in contrast to *in vivo* data that extremely weak Ni^{2+} peaks were observed. However, in the presence of increasing amounts of Bi³⁺, a Bi³⁺ peak appeared and increased its intensities at an elution time corresponding to *Hp*HypA dimer accompanied by the reduction of the Zn^{2+} peak intensities at *Hp*HypA monomer and almost

complete displacement of Zn^{2+} at a molar ratio of [Bi³⁺]/[HypA] of 1.0. In the meantime, a gradual shift of Ni^{2+} peaks from *Hp*HypA monomer to its dimer is evident (Fig. 4E, Fig. S11). Nevertheless, the total amounts of Ni^{2+} bound to *Hp*HypA remained unchanged under Bi³⁺ stress, in agreement with the direct ICP-MS quantification results, but in sharp contrast to *in vivo* observation.
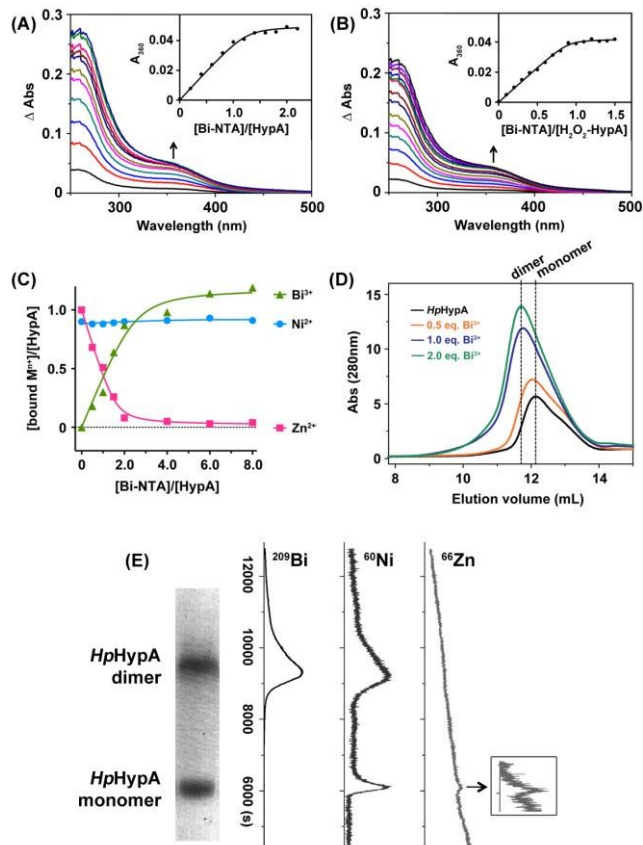

Fig. 4 Binding of Bi³⁺ to recombinant *Hp*HypA. UV-vis difference spectra of *Hp*HypA (A) and H_2O_2-treated *Hp*HypA (B) upon addition of different molar equivalents of Bi-NTA. The *insets* show titration curves at 360 nm. (C) Molar ratios of bound Zn^{2+}, Ni^{2+} and Bi³⁺ over *Hp*HypA upon incubation of Ni, Zn-HypA with different molar equivalents of Bi-NTA. (D) Size-exclusion chromatography (Superdex 75 10/300 GL) profiles of *Hp*HypA incubated with 0.5, 1.0 and 2.0 molar equivalents of Bi-NTA. (E) GE-ICP-MS analysis of purified Ni, Zn-*Hp*HypA upon incubation with 1 molar equivalent of Bi-NTA. The corresponding *Hp*HypA dimer and monomer separated by a slab gel is shown for comparison. *Inset*: zoom in of the ICP-MS spectra of ⁶⁶Zn associated with *Hp*HypA monomer.

Intracellular metal selectivity of *Hp*HspA

E. coli cells overexpressing *Hp*HspA were cultured in M9 medium in the presence of different metal ions. Different from *Hp*HypA, *Hp*HspA was expressed at a similar level under all conditions as revealed by SDS-PAGE (Fig. S2). The GE-ICP-MS analysis of the cell lysates gave rise to four metal peaks observable at almost the same elution times, corresponding to the heptamer of *Hp*HspA (Fig. 5A). Subsequent MS-based peptide mass fingerprinting analysis revealed that *Hp*HspA is the only protein identified in the fractions corresponding to the major metal peaks (Table S4). Of the seven metals monitored, Co^{2+},

Ni^{2+}, Cu^{2+} and Zn^{2+} were detected to bind *Hp*HspA with a total of *ca.* 0.5 molar equivalents of metals bound per *Hp*HspA monomer (Table S5). Amongst all the bound metal ions, Zn^{2+} appeared to be the most favored one, which accounted for 69%, followed by Co^{2+}, Ni^{2+} and Cu^{2+} with fractions of 14%, 13% and 4% respectively (Fig. 5B).

Upon supplementation to the cell cultures with bismuth (as Bi-NTA) at concentrations up to 20 μM under identical conditions, the total amounts of metal ions bound to *Hp*HspA remained almost unchanged, but the proportions of metals bound to *Hp*HspA were altered with the fractions of Zn^{2+}, Ni^{2+}, Co^{2+} decreased obviously to 35%, 2% and 4% respectively. In contrast, the amounts of Cu^{2+} and Bi^{3+} bound to the protein increased with the increase in Bi^{3+} concentrations (Fig. 5C, Table S5). The results indicate that Bi^{3+} might inhibit *Hp*HspA to acquire its cognate metal cofactors such as Ni^{2+} and Zn^{2+} in cells, thus disrupting the function of *Hp*HspA.
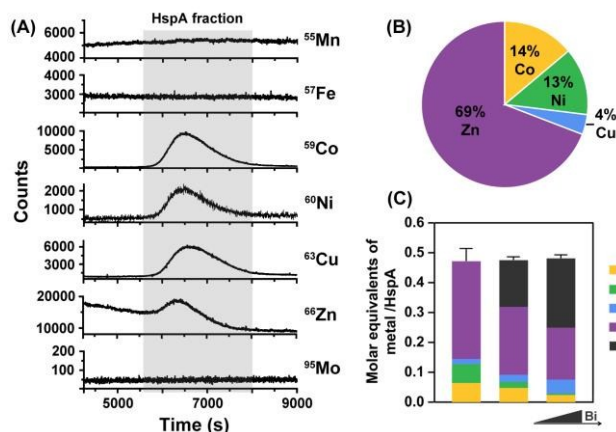

Fig. 5 Metal selectivity of *Hp*HspA in *E. coli* cells. (A) GE-ICP-MS profiles of various metals associated with *Hp*HspA. (B) Distribution of metals associated with *Hp*HspA. (C) Distribution of metals associated with *Hp*HspA under the stress of Bi^{3+} at different concentrations. *E. coli* cells harboring *hspA* gene were grown in M9 medium supplemented with seven metals (10 μM each) with or without 10 or 20 μM of Bi^{3+}.

Unexpectedly, we also observed that *Hp*HspA associated with toxic metal Pb^{2+} when overexpressed in LB medium (Fig. S12), though Pb^{2+} contents in the medium are extremely low (0.01 μM, *ca.* 0.01% of total metals in LB medium).[3] Unlike *Hp*HypA which exhibits high specificity towards Zn^{2+}, *Hp*HspA may serve as a metal reservoir and binds a range of metal ions inside cells.

Discussion

Bacterial metalloproteins have been evolved to maintain cellular metal homeostasis *via* elaborate mechanisms.[27] Overall, the functionality of a metalloprotein depends on its ability to obtain the right metal cofactors. Given the complexity of cellular environments (intracellular reducing environment), metal selectivity and metal binding properties of a metalloprotein should not be simply characterized by *in vitro* investigation of a purified protein, as a protein may bind to a series of metal ions *in vitro*. Indeed, the *in vivo* metal selectivities of certain metalloproteins are distinct from those observed *in vitro* according to several recent in-cell NMR studies.[30-32] Hence, a methodology that can be used to unveil the cellular protein

metallation profiles is desirable for understanding the physiological role of a given metalloprotein.

We have recently developed a strategy by on-line coupling of continuous-flow gel electrophoresis with ICP-MS (GE-ICP-MS) to allow cellular metal ions and their bound proteins to be tracked simultaneously.[3] Here, we further examine the feasibility of the approach in quantitative analysis of intracellular metal-protein binding properties including stoichiometry and selectivity. Despite that the metal-protein complexes at dissociation constants (K_d) ranging from 10^{-12} M (Cu-BSA) to 10^{-21} M (Fe-Tf) (Table S2) are well preserved during gel electrophoresis,[3] it is not clear whether this is the case when dissociation constants drop to micromolars, which are commonly found for many metal-metallochaperone interactions. We selected HypA and HspA from *H. pylori* as showcases since they are well-studied Ni^{2+} accessory proteins. Both of them bind a range of metal ions with diverse affinities facilitating nickel-enzyme maturation in *H. pylori* (Table S2). Moreover, their capabilities of binding to transition metal ions are susceptible to change under the stress of metallodrugs such as bismuth-based anti-ulcer drugs.[8, 10] GE-ICP-MS analysis of purified Zn,Ni-*Hp*HypA gave rise to low metal recovery under the assumption that the protein amounts remained unchanged. However, when sulfur (^{34}S) was determined in parallel with metals and used to quantify the protein amounts, almost stoichiometric bindings of both Zn^{2+} and Ni^{2+} to *Hp*HypA were obtained, suggesting substantial losses of proteins (*ca.* 40% for *Hp*HypA) during GE-ICP-MS analysis. In addition, an excellent linearity (> 0.99) between the measured and initially added amounts of both Zn^{2+} and Ni^{2+} that bind to *Hp*HypA was observed for GE-ICP-MS analysis (Fig. 1). Our combined data clearly demonstrate that GE-ICP-MS analysis is able to retain the integrity of metal-protein complexes with dissociation constants at nano-molars for Zn-*Hp*HypA, and micro-molars for Ni-*Hp*HypA.

Due to protein losses during GE-ICP-MS analysis, quantification of protein amounts is critical for determination of intracellular metal-protein stoichiometry precisely. For metalloprotein quantification using GE-ICP-MS system, parallel measurements of sulfur and metals enabled us to simultaneously quantify both the protein and its bound metal contents, thus eliminating the quantitative inaccuracy due to protein losses during gel electrophoresis. Both internal and external calibration methods were applicable to determine intracellular protein amount, providing that the sulfur amounts of the external standard is precisely known. Although the sensitivity of ^{34}S measured by ICP-MS is not ideal owing to lack of an octopole reaction system (ORS) in the instrument, the external sulfur calibration by multiple injection of protein standards still yields a good linearity (^{34}S with $R^2 > 0.99$, Fig. S3), demonstrating the feasibility of accurate protein quantification *via* monitoring ^{34}S signals in GE-ICP-MS.

We then used GE-ICP-MS to examine intracellular metal selectivity of the metallochaperones HypA and HspA towards a series of metal ions supplemented in the culture medium at concentrations of 10 μM, which are in excess compared with the overexpressed levels of *Hp*HypA and *Hp*HspA in cells (estimated to be 1.01(±0.12) and 5.46(±0.86) μM in 100 mL culture medium respectively) (Fig. S13). Interestingly, *Hp*HypA exhibits extremely high specificity in cells towards its structural metal ion and failure to provide Zn^{2+} in the culture medium led to no overexpression of the protein (Fig. S1). Such a highly specific metal-protein interaction in cells was also observed previously in hSOD1, which binds stoichiometric zinc only in its native zinc site but not the copper site, different from *in vitro*

observation that two zinc ions occupy both metal sites of hSOD1.[31, 32] In contrast, *Hp*HspA, similar to *Hp*SlyD,[3] does not exhibit high specificity in cells towards transition metal ions and simultaneously binds Zn^{2+}, Ni^{2+}, Co^{2+} and Cu^{2+}, with Zn^{2+} being the most favored metal ion (Fig. 5). In addition, it also binds Pb^{2+}. HspA from *H. pylori* possesses a unique cysteine- and histidine-rich metal binding domain at the C-terminus. It might serve as a metal reservoir to sequester metal ions or undergo metal exchange with other proteins,[1] resembling the cysteine-rich metallothioneins, which play crucial roles in cellular metal storage and redistribution given that changes in the thiol-disulfide redox states confer kinetic liability to their transient metal binding sites.[33, 34]

Unexpectedly, only *ca* 3% Ni^{2+} binds to *Hp*HypA overexpressed in *E. coli* (Table 2 and Table S6), distinct from stoichiometric binding of this metal found *in vitro*.[35] Although cautions shall be taken when interpreting the results as the metalloprotein is overexpressed from a heterologous expression system, the inherent property of a metal binding site often plays a key role in metal selectivity of a metalloprotein.[26] Therefore, we suggest that Ni^{2+} might bind to *Hp*HypA transiently under physiological conditions. This was further verified by subsequent intracellular metal accumulation data that the amounts of Zn^{2+} increased significantly compared with that of Ni^{2+} upon *Hp*HypA overexpression (Fig. 2A), and such a transient metal-protein interaction often occurs in cells.[1]

Bismuth compounds have been used in clinic for the treatment of *H. pylori* infection for decades.[29, 36-40] Increasing evidence have shown that Bi^{3+} binds to proteins and enzymes from *H. pylori* and is able to displace metal ions such as Zn^{2+} or Ni^{2+} from key metalloenzymes, thus disrupting their functions.[10, 16, 41] Although *Hp*HypA exhibited high specificity towards Zn^{2+} in cells, binding of Zn^{2+} to the protein was completely abolished under the stress of higher concentrations (> 40 μM) of Bi^{3+} (Fig. 3). Binding of Ni^{2+} to both *Hp*HypA and *Hp*HspA was inhibited upon supplementation of even 10 μM Bi^{3+} to cell culture medium. It is likely that Bi^{3+} binds to the Ni^{2+} site of *Hp*HspA at its C-terminus rich in histidines and cysteines,[8] similar to another nickel-chaperone *Hp*HypB with its Ni^{2+} site being replaced by Bi^{3+}.[10] Given that Ni^{2+} binds to *Hp*HypA with a square planar geometry through Met1, His2, Glu3 and Asp40,[12] it is unlikely that Bi^{3+} can displace Ni^{2+} from the protein, which is also supported by our *in vitro* study. The disrupted Ni^{2+} binding *in vivo* might result from a global effect of Ni^{2+} deficiency in cells in the presence of Bi^{3+} (Fig. S14). This suggests that *in vitro* observation might not reflect real situation in complex biological systems and the intracellular metal selectivity might be distinct for individual metalloproteins.

Conclusions

We validate that GE-ICP-MS is a feasible method for quantitative analysis of intracellular metal-protein interactions including stoichiometry and metal selectivity providing that metal and sulphur signals are simultaneously detected. Using this technique, we provide new aspects of metal binding properties of the two metallochaperones *Hp*HypA and *Hp*HspA overexpressed in *E. coli* cells, distinct from *in vitro* observations. GE-ICP-MS might serve as a generalized approach to allow various metals and their associated proteins to be quantitatively examined inside cells and also add additional dimension in SDS-PAGE gel. We anticipate that the current approach will play a role in microbial and human metallomics.[22, 42-44]

Address

Department of Chemistry, The University of Hong Kong, Pokfulam Road, Hong Kong, P. R. China

E-mail: hsun@hku.hk; Fax: +852 2857-1586.

Notes and References

1. W. Maret, *Metallomics*, 2010, **2**, 117-125.
2. D. Profrock and A. Prange, *Appl. Spectrosc.*, 2012, **66**, 843-868.
3. L. Hu, T. Cheng, B. He, L. Li, Y. Wang, Y. T. Lai, G. Jiang and H. Sun, *Angew. Chem. Int. Ed.*, 2013, **52**, 4916-4920.
4. L. A. Finney and T. V. O'Halloran, *Science*, 2003, **300**, 931-936.
5. S. Tottey, D. R. Harvie and N. J. Robinson, *Acc. Chem. Res.*, 2005, **38**, 775-783.
6. L. Banci, I. Bertini, S. Ciofi-Baffoni, T. Kozyreva, K. Zovo and P. Palumaa, *Nature*, 2010, **465**, 645-648.
7. H. M. Alvarez, Y. Xue, C. D. Robinson, M. A. Canalizo-Hernández, R. G. Marvin, R. A. Kelly, A. Mondragón, J. E. Penner-Hahn and T. V. O'Halloran, *Science*, 2010, **327**, 331-334.
8. S. Cun and H. Sun, *Proc. Natl. Acad. Sci. USA*, 2010, **107**, 4943-4948.
9. M. E. Palm, C. F. Weise, C. Lundin, G. Wingsle, Y. Nygren, E. Björn, P. Naredi, M. Wolf-Watz and P. Wittung-Stafshede, *Proc. Natl. Acad. Sci. USA*, 2011, **108**, 6951-6956.
10. W. Xia, H. Li and H. Sun, *Chem. Commun.*, 2014, **50**, 1611-1614.
11. W. Xia, H. Li, X. Yang, K. B. Wong and H. Sun, *J. Biol. Chem.*, 2012, **287**, 6753-6763.
12. W. Xia, H. Li, K.-H. Sze and H. Sun, *J. Am. Chem. Soc.*, 2009, **131**, 10031-10040.
13. X. Yang, H. Li, T. Cheng, W. Xia, Y. T. Lai and H. Sun, *Metallomics*, 2014, **6**, 1731-1736.
14. A. M. Sydor, H. Lebrette, R. Ariyakumaran, C. Cavazza and D. B. Zamble, *J. Biol. Chem.*, 2014, **289**, 3828-3841.
15. X. Yang, H. Li, T. P. Lai and H. Sun, *J. Biol. Chem.*, 2015, doi: 10.1074/jbc.M1114.632364.
16. S. Cun, H. Li, R. Ge, M. C. Lin and H. Sun, *J. Biol. Chem.*, 2008, **283**, 15142-15151.
17. K. Schauer, C. Muller, M. Carriere, A. Labigne, C. Cavazza and H. De Reuse, *J. Bacteriol.*, 2010, **192**, 1231-1237.
18. R. Ge, X. Sun, Q. Gu, R. M. Watt, J. A. Tanner, B. C. Wong, H. H. Xia, J. D. Huang, Q. Y. He and H. Sun, *J. Biol. Inorg. Chem.*, 2007, **12**, 831-842.
19. T. Cheng, H. Li, W. Xia and H. Sun, *J. Biol. Inorg. Chem.*, 2012, **17**, 331-343.
20. H. Kaluarachchi, J. F. Siebel, S. Kaluarachchi-Duffy, S. Krecisz, D. E. Sutherland, M. J. Stillman and D. B. Zamble, *Biochemistry*, 2011, **50**, 10666-10677.
21. M. K. Tse, C. K. Cho, W. F. Wong, B. Zou, S. K. Hui, B. C. Wong and K. H. Sze, *Protein Sci.*, 2012, **21**, 1418-1428.
22. S. Mounicou, J. Szpunar and R. Lobinski, *Chem. Soc. Rev.*, 2009, **38**, 1119-1138.
23. M. Garijo Añorbe, J. Messerschmidt, I. Feldmann and N. Jakubowski, *J. Anal. At. Spectrom.*, 2007, **22**, 917-924.
24. Y. N. Ordóñez, C. L. Deitrich, M. Montes-Bayón, E. Blanco-González, J. Feldmann and A. Sanz-Medel, *J. Anal. At. Spectrom.*, 2011, **26**, 150-155.
25. Y. Nakatani, T. Kleffmann, K. Linke, Stephen M. Condon, Mark G. Hinds and Catherine L. Day, *Biochem. J.*, 2013, **450**, 629-638.
26. A. W. Foster and N. J. Robinson, *BMC Biol.*, 2011, **9**, doi: 10.1186/1741-7007-9-25.
27. K. J. Waldron, J. C. Rutherford, D. Ford and N. J. Robinson, *Nature*, 2009, **460**, 823-830.

28. H. Sun, H. Li, I. Harvey and P. J. Sadler, *J. Biol. Chem.*, 1999, **274**, 29094-29101.

29. H. Li and H. Sun, *Curr. Opin. Chem. Biol.*, 2012, **16**, 74-83.

30. J. A. Hubbard, L. K. MacLachlan, G. W. King, J. J. Jones and A. P. Fosberry, *Mol. Microbiol.*, 2003, **49**, 1191-1200.

31. L. Banci, L. Barbieri, I. Bertini, F. Cantini and E. Luchinat, *PlosOne*, 2011, **6**, e23561, doi: 10.1371/journal.pone.0023561.

32. L. Banci, L. Barbieri, I. Bertini, E. Luchinat, E. Secci, Y. Zhao and A. R. Aricescu, *Nat. Chem. Biol.*, 2013, **9**, 297-299.

33. D. E. K. Sutherland and M. J. Stillman, *Metallomics*, 2011, **3**, 444-463.

34. P. Babula, M. Masarik, V. Adam, T. Eckschlager, M. Stiborova, L. Trnkova, H. Skutkova, I. Provaznik, J. Hubalek and R. Kizek, *Metallomics*, 2012, **4**, 739-750.

35. A. Atanassova and D. B. Zamble, *J. Bacteriol.*, 2005, **187**, 4689-4697.

36. H. Sun, *Biological Chemistry of Arsenic, Antimony and Bismuth*, John Wiley & Sons, 2011.

37. R. Ge and H. Sun, *Acc. Chem. Res.*, 2007, **40**, 267-274.

38. N. Yang and H. Sun, *Coord. Chem. Rev.*, 2007, **251**, 2354-2366.

39. N. P. Barry and P. J. Sadler, *Chem. Commun.*, 2013, **49**, 5106-5131.

40. K. M. Fock, D. Y. Graham and P. Malfertheiner, *Nat. Rev. Gastroenterol. Hepatol.*, 2013, **10**, 495-500.

41. L. Zhang, S. B. Mulrooney, A. F. Leung, Y. Zeng, B. B. Ko, R. P. Hausinger and H. Sun, *BioMetals*, 2006, **19**, 503-511.

42. S. M. Yannone, S. Hartung, A. L. Menon, M. W. Adams and J. A. Tainer, *Curr. Opin. Biotechnol.*, 2012, **23**, 89-95.

43. H. Sun and Z.-F. Chai, *Annu. Rep. Prog. Chem., Sect. A*, 2010, **106**, 20-38.

44. X. Sun, C.-N. Tsang and H. Sun, *Metallomics*, 2009, **1**, 25-31.